

# Electronic and Cytotoxic Properties of 2-Amino-naphtho[2,3-*b*]furan-4,9-diones

Sandra Jiménez-Alonso,<sup>†,‡</sup> Judith Guasch,<sup>§</sup> Ana Estévez-Braun,<sup>\*,†,‡</sup> Imma Ratera,<sup>§</sup> Jaume Veciana,<sup>\*,§</sup> and Angel G. Ravelo<sup>\*,†,‡</sup>

<sup>†</sup>Instituto Universitario de Bio-Organica "Antonio González", Universidad de La Laguna, Avda. Astrofísico Fco. Sánchez, 38206 La Laguna, Tenerife, Spain

<sup>‡</sup>Instituto Canario de Investigaciones del Cáncer (ICIC)

<sup>§</sup>Department of Molecular Nanoscience and Organic Materials, Institut de Ciència de Materials de Barcelona (CSIC), Universitat Autònoma de Barcelona and CIBER de Bioingeniería, Biomateriales y Nanomedicina (CIBER-BBN), 08193 Bellaterra, Barcelona, Spain

**S** Supporting Information

**ABSTRACT:** The electronic properties of a new set of cytotoxic 2-amino-naphtho[2,3-*b*]furan-4,9-dione derivatives (**1–8**) are evaluated. The electron delocalization of these compounds is described by means of their redox potentials and solvatochromic properties. The large solvatochromism of their intramolecular electron transfer band is analyzed using the linear solvation energy relationship method. In addition, this method determined the importance of the molecular environment, quantifying the interactions that compounds (**1–8**) establish with their surrounding media, with the capacity of acting as hydrogen-bond acceptors (HBA) and hydrogen-bond donors (HBD) and the dipolarity/polarizability being the most significant ones. As a result, a relationship between the electronic and the cytotoxic properties of these compounds is proposed.

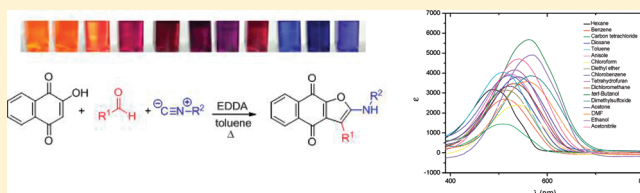


**Figure 1.** Redox cycling process of quinone.

reactive oxygen species, which can cause additional damage to the DNA.<sup>14</sup>

Another transformation is mainly found in the cytoplasm of tissues, is catalyzed by the enzyme NAD(P)H:quinone oxidoreductase, and involves a two-electron reduction of the quinone function producing hydroquinone using either NADH or NADPH as electron donor. This intermediate may then be inactivated by a subsequent glucuronidation and/or sulfation or by the conversion of the hydroquinone into an alkylating intermediate, the quinone methide. Two-electron reduction is

Quinones are organic compounds of major importance in biological systems and industrial applications as dyes or drugs.<sup>1</sup> Compounds with quinone cores are common in nature and play important physiological roles in animals and plants.<sup>2</sup> They are used in anticancer,<sup>3</sup> antibacterial,<sup>4</sup> and antimalarial<sup>5</sup> drugs and as fungicides.<sup>6</sup> On the basis of their numerous biological activities and structural properties, this scaffold is considered a privileged structure in medicinal chemistry.<sup>7,8</sup> Quinones are oxidants and electrophiles. Since a nucleophilic addition to a quinone represents a formal two-electron reduction, these properties are interrelated.<sup>9</sup> Hence, they play a major role as bioreductive drugs, oxidative stress enhancers, and redox catalysts.<sup>10</sup> Two major mechanisms of cytotoxicity have been proposed: stimulation of oxidative stress and alkylation of cellular nucleophiles, which encompass a large range of biomolecules.<sup>11</sup> Quinones undergo reversible oxidation–reduction processes (Figure 1) generating reactive oxygen species (ROS) such as superoxide ( $O_2^{\cdot-}$ ) and hydrogen peroxide ( $H_2O_2$ ), causing oxidative stress and inducing DNA damage to some essential proteins.<sup>12</sup>

Under aerobic conditions, i.e., in tumors with sufficient blood supply, a one-electron reduction predominates, resulting in free-radical intermediates that can react with molecular oxygen and ensuing superoxide production.<sup>13</sup> The superoxide anion radical is further metabolized to hydrogen peroxide ( $H_2O_2$ ) and other

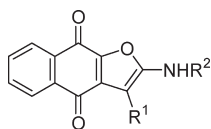


**Figure 2.** Structure of 2-amino-naphtho[2,3-*b*]furan-4,9-dione derivatives.

generally known as the detoxification step by reducing the quinone into the stable hydroquinone, which is readily excreted after conjugation. Such a pattern is believed to predominate under anaerobic conditions or inside anaerobic *loci* within a cell.

However, to obtain more information about the mechanisms of cytotoxicity it is interesting to study not only the electronic properties of the bioactive quinones but also their molecular environment. Changes of the intermolecular interactions (hydrogen-bond ability, dipolar moment, etc.) are clearly capable of affecting the structures, reactivities, biological activities, equilibria, reaction rate constants, and a host of other aspects that are of central interest to chemistry and biology.<sup>15</sup> Electrochemical and spectroscopic measurements are well suited for characterizing the molecules in their local environment.<sup>16</sup> Thus, specific shifts in the redox potentials and in the absorption spectra reflect the extent of stabilization that the molecular ground and excited states experience due to their own nature as well as their solvent–solute interactions.<sup>17</sup>

Our research group is especially interested in antitumoral compounds based on quinone cores fused to heterocyclic rings.<sup>5,8c–8f</sup> In this sense, we have recently published the design and synthesis of novel pyranonaphthoquinones through an intramolecular domino Knoevenagel hetero-Diels–Alder reaction. The obtained adducts resulted to be effective catalytic inhibitors of topoisomerase II.<sup>8d</sup>

With the aim of obtaining new bioactive quinones, we synthesized a set of new 2-amino-naphtho[2,3-*b*]furan-4,9-dione derivatives (Figure 2). These compounds were tested for cytotoxicity against several human solid tumor cell lines (MCF7, MCF7/BUS, and SK-Br-3). Moreover, the electronic properties of these aromatic donor–acceptor derivatives were analyzed by means of their redox potentials and solvatochromic properties. This study revealed that the higher the electron delocalization within the molecule, the higher the cytotoxicity against the tested human solid tumor cell lines. In addition, thanks to the linear solvation energy relationship method applied to determine the solvatochromism of these compounds, we were able to identify the interactions that the molecules establish with their environment.

## RESULTS AND DISCUSSION

**Synthesis and Cytotoxic Activity.** 2-Amino-naphtho[2,3-*b*]furan-4,9-diones (1–8) were synthesized using a one-pot

three-component reaction following a modified methodology described by Temouri et al.<sup>18</sup> Thus, the reaction of 2-hydroxynaphthoquinone with various aldehydes and aromatic or aliphatic isocyanides, under refluxing in toluene, afforded the corresponding 2-amino-naphtho[2,3-*b*]furan-4,9-dione (Figure 3). The synthesis of linear naphtho[2,3-*b*]furan-4,9-dione derivatives can be rationalized by the initial formation of a conjugated electron-deficient enone (A) through a Knoevenagel condensation of the 2-hydroxy-1,4-naphthoquinone and an aldehyde. The next step of this mechanism could involve a [4 + 1] cycloaddition reaction of the electron-deficient heterodiene moiety of the adduct (A) with the isocyanide to afford an iminolactone intermediate (B). The subsequent isomerization of iminolactone (B) leads to the formation of the corresponding naphthofuran derivative. The use of EDDA as a catalyst accelerated the process and afforded the desired products in higher yields and shorter times.

The structures of the new 2-amino-naphtho[2,3-*b*]furan-4,9-diones (1–8) and the corresponding reaction yields are detailed in Table 1. Good yields were obtained when aliphatic or aromatic aldehydes were used. The worst yield (57%) resulted from the combination of the hindered *tert*-butyl isocyanide with benzaldehyde.

An intense solvatochromic effect was detected during the manipulation of the obtained compounds with different solvents, and all products were isolated as amorphous deep blue solids. As an example, single crystals of 3 were grown by slow evaporation from acetone and used for their X-ray crystal determination. Weak H-bonds were found between the amino proton and the carbonyl groups of neighboring quinones leading to a distance of 2.44 Å between molecules (Figure 4).

To determine the potential cytotoxicity of these derivatives according to antecedents of different naphthoquinones,<sup>19</sup> compounds 1–8 were tested against the following tumoral cell lines: MCF7, MCF7/BUS, and SK-Br-3 (Table 2).

Compounds 4, 6, and 8 exhibit the highest cytotoxicities. Compound 4 shows selectivity toward the hormone-dependent cell line MCF7/BUS with a GI<sub>50</sub> value of 9.2 μM. Compounds 6 and 8 present good cytotoxicities against MCF7, MCF7/BUS, and SK-Br-3 tumor cell lines. The best GI<sub>50</sub> was achieved by compound 6 against the SK-Br-3 cell line, with GI<sub>50</sub> = 1.6 μM.

**Electrochemistry.** The electrochemistry of a plethora of quinones has been widely studied.<sup>13</sup> However, there are only few reports on electrochemical studies of heterocyclic naphthoquinones.<sup>9c</sup> Cyclic voltammograms of naphthoquinones in organic aprotic solvents present two typical waves corresponding to two sequential reversible or quasi-reversible one-electron transfer processes (Figure 5). The first wave is related to the redox couple quinone (Q)/semiquinone anion radical (Q<sup>•-</sup>), whereas the second one is related to the semiquinone anion radical (Q<sup>•-</sup>)/quinone dianion (Q<sup>2-</sup>).<sup>20</sup>

In our case, cyclic voltammograms of the 2-amino-naphtho[2,3-*b*]furan-4,9-dione derivatives were performed in DMF using tetrabutylammonium hexafluorophosphate (HFPTBA)

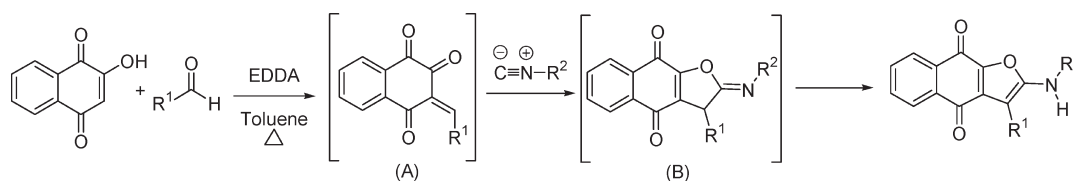


**Figure 3.** Synthesis of compounds (1–8) through a one-pot three-component reaction.

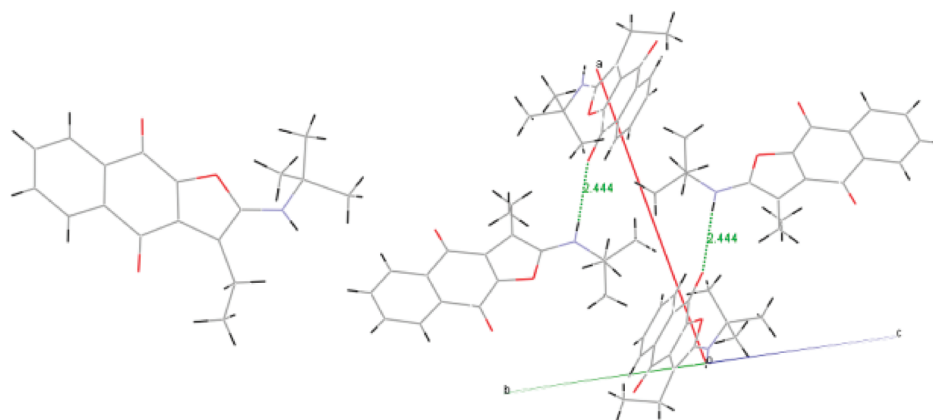


Figure 4. Crystal structure and packing of compound 3.

Table 1. Summary of the Synthesis of 2-Amino-naphtho[2,3-*b*]furan-4,9-dione Derivatives (1–8)

Entry	Aldehyde	Isocyanide	Product	Yield %
1				77
2				94
3				90
4				79
5				57
6				96
7				89
8				97

as supporting electrolyte under different scan rates (50–125 mV s<sup>-1</sup>). The obtained potential values are referred to Fc/Fc<sup>+</sup>, as recommended by IUPAC, and all studies were carried out in an inert

Table 2. Cytotoxic Activity of Compounds 1–8 against a Representative Panel of Human Breast Cancer Cell Lines<sup>a</sup>

compound	MCF7	MCF7/BUS	SK-Br-3
1	18.8 (±0.07)	12.1 (±0.6)	10.2 (±0.3)
2	29.8 (±0.4)	15.2 (±0.4)	14.6 (±0.5)
3	29.9 (±1.3)	17.9 (±0.4)	24.5 (±1.5)
4	22.2 (±1.2)	9.22 (±0.4)	22.9 (±2.0)
5	82.0 (±2.5)	95.2 (±0.9)	87.8 (±2.4)
6	5.9 (±0.4)	2.8 (±0.5)	1.6 (±0.4)
7	19.4 (±0.4)	17.4 (±0.6)	14.1 (±0.3)
8	7.6 (±0.4)	3.9 (±0.07)	5.8 (±0.6)

<sup>a</sup> Expressed as GI<sub>50</sub> values given in μM and determined as means of two to five experiments; standard deviations are given in parentheses.

atmosphere by saturation with argon during several minutes at room temperature. As expected, these molecules exhibit two waves, the Q/Q<sup>•-</sup> reversible and the Q<sup>•-</sup>/Q<sup>2-</sup> quasi-reversible (Figure 6).

The residual water present in the solvent might catalyze the disproportionation of the radical anion or be reduced by the electrogenerated dianion (Q<sup>2-</sup>),<sup>21</sup> explaining the quasi-reversible character of the second reduction process. It could also be explained as being due to the ion-pairing stabilization of the quinone dianion (Q<sup>2-</sup>) by the tetrabutylammonium cation.<sup>22</sup> Taking into account the nature of the two waves, the discussion refers only to the reversible wave I (Table 3).

The presence of an aromatic moiety in the structure of the 2-amino-naphtho[2,3-*b*]furan-4,9-dione derivatives favors the delocalization of their electrons. Moreover, as reported for aromatic dianions,<sup>23</sup> charges dispersed over a large molecular framework are usually less affected or unaffected by counterions. Consequently, compounds 5, 6, 7, and 8 present higher redox potentials than the rest and therefore, their reductions are facilitated ( $E_{1/2}^I > -1,300$  V). It is interesting to highlight that compounds 5 and 6, which exhibit the best electron delocalization due to the presence of an aromatic group directly attached to the carbon C-3 of the furan ring, have the highest reduction potentials. Another crucial factor to take into account for compound 6 is its extra stabilization caused by the formation of an intramolecular seven-membered ring between the 2'-H (furan numbering) and one oxygen of the quinone structure (Figure 7).

This O–H interaction reduces the electron density on the oxygen, increases the electrophilic nature of the aromatic system,

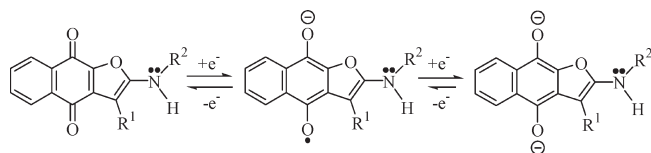


**Figure 5.** Scheme of the redox processes of the 2-amino-naphtho[2,3-*b*]furan-4,9-dione derivatives.

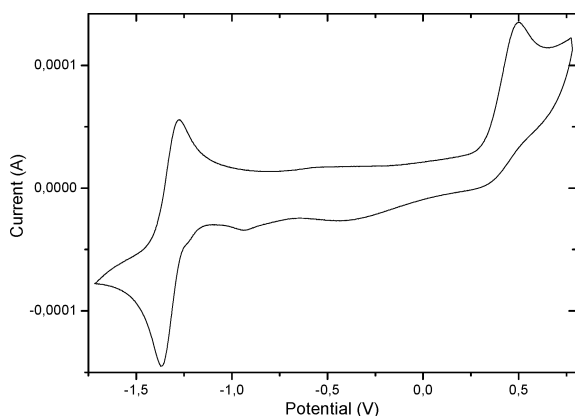


**Figure 6.** Cyclic voltammogram of **3** (wave I:  $Q/Q^{\cdot-}$ ; wave II:  $Q^{\cdot-}/Q^{2-}$ ).  $[Q] = 1.0$  mM in DMF/HFPTBA (0.1 M);  $25$  °C;  $\nu = 0.1$  V  $s^{-1}$ .

**Table 3.** Voltammetric Parameters of **1–8** vs  $Fc/Fc^{+a}$

	wave I				wave II	
	$E_a^I$ (V)	$E_c^I$ (V)	$\Delta E^I$ (V)	$E_{1/2}^I$ (V)	$I_a/I_c^I$	$E_a^{II}$ (V)
<b>1</b>	-1.2977	-1.3903	0.0926	-1.3440	0.86	0.4134
<b>2</b>	-1.3017	-1.3780	0.0764	-1.3398	0.80	0.3987
<b>3</b>	-1.2779	-1.3742	0.0963	-1.3260	0.98	0.4246
<b>4</b>	-1.2606	-1.3891	0.1285	-1.3248	0.90	0.4392
<b>5</b>	-1.2523	-1.3379	0.0856	-1.2951	0.96	0.4610
<b>6</b>	-1.2018	-1.3030	0.1012	-1.2524	0.71	0.4660
<b>7</b>	-1.2432	-1.3635	0.1202	-1.3033	0.55	0.4767
<b>8</b>	-1.2339	-1.3621	0.1282	-1.2980	0.62	0.4070

<sup>a</sup>  $[Q] = 1.0$  mM in DMF/HFPTBA 0.1 M;  $25$  °C;  $\nu = 0.1$  V  $s^{-1}$ .

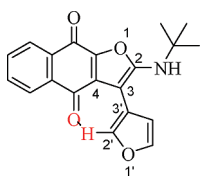


**Figure 7.** H-bonding interaction between the furan ring and the carbonyl group in compound **6**.

and stabilizes the semiquinone anion radical formed during the intramolecular electron transfer process (IET) that these compounds present (Figure 8).<sup>13,24</sup> Obviously, this interaction can also take place in the other compounds but is favored in compound **6** thanks to the electron-withdrawing oxygen element of the furan ring. Compounds without aromatic groups directly bonded to the furano-naphthoquinone structure present lower redox potentials all of them being  $E_{1/2}^I < -1,300$  V. Finally, it is worth to mention that the presence of atmospheric oxygen in the sample modifies the cyclic voltam-

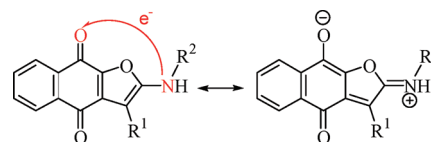


**Figure 8.** Neutral and zwitterionic resonance formulas of 2-amino-naphtho[2,3-*b*]furan-4,9-dione derivatives (the neutral form dominates in the electronic ground state, and the dipolar zwitterionic form dominates in the CT excited state).

grams. The expected ones can be obtained after degasification with argon, which demonstrates the reversibility of the involved process and the stability of these compounds after reacting with oxygen.

According to these results, the 2-amino-naphtho[2,3-*b*]furan-4,9-dione derivatives with the higher electron delocalizations present higher reduction potentials and higher cytotoxic activities against the studied cell lines, as already observed in other similar systems.<sup>25</sup> High reduction potentials facilitate the semiquinone formation and therefore the initial bioreduction step described in many cytotoxic mechanisms of action of different naphthoquinones. Moreover, the influence of the oxygen observed in the cyclic voltammograms supports the importance of this factor as previously reported,<sup>26</sup> as well as the mechanism of action related to reactive oxygen species. Consequently, although caution must be taken in interpreting these results, it is reasonable to think that a plausible mechanism of action of these compounds involves an initial bioreduction process followed by the generation of reactive oxygen species. Moreover, 2-amino-naphtho[2,3-*b*]furan-4,9-dione derivatives with  $E_{1/2}^I > -1,250$  V are very susceptible to show cytotoxic activity against the MCF7, MCF7/BUS, and SK-Br-3 cell lines. However, even though the trend between the redox potentials and the cytotoxicities of these compounds is clear, it was not possible to establish an unequivocal lineal relationship between these parameters pointing out the importance of other factors such as steric, lipophilic, etc. of *in vitro* cytotoxicity. Compound **5**, with an aromatic substituent, is the only product that having a high redox potential shows a low cytotoxic activity. This fact indicates that compound **5** possibly acts through a different mechanism or presents other properties that are significant for its cytotoxicity.

**Intramolecular Electron Transfer Process and Its Solvent Dependence.** It is known that the molecular environment and the different intermolecular interactions are very important for bioactive compounds. They affect parameters such as diffusion, solubility, and membrane permeability, among others.<sup>27</sup> To study the molecular environment, spectroscopic measurements were used. The solvatochromic shifts related to the intramolecular electron transfer (IET) process (Figure 8) were studied using an empirical method called linear solvation energy relationship (LSER), developed by Kamlet, Taft, and co-workers.<sup>28</sup> This method not only determines the media effect in terms of specific solvent–solute interactions, such as possible solvation spheres that surround the molecules and affect their capacity of bonding with the substrates, but also gives an alternative approach to the cyclic voltammetry technique to quantify the electronic properties of such molecules. Therefore, the LSER method is extremely suitable to analyze the electronic properties of the 2-amino-naphtho[2,3-*b*]furan-4,9-diones to relate them to their cytotoxic activity.

Marcus theory for donor–acceptor (DA) systems makes it possible to correlate the energy of the optical absorption due to a charge transfer (CT) ( $E_{opt}$  or  $h\nu_{max}$ ) with the free energy changes that the molecule experiences during the charge separa-



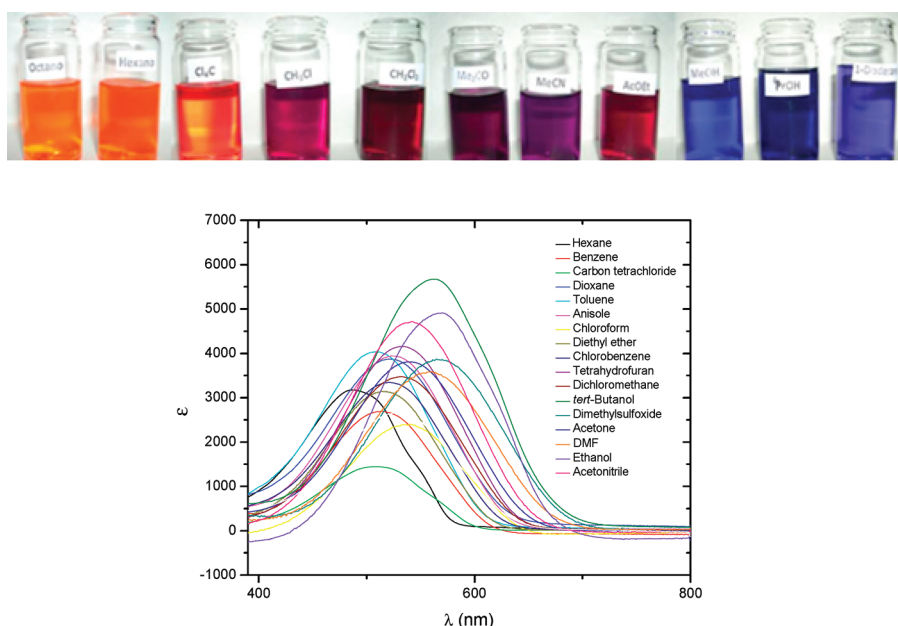


**Figure 9.** (Top) Solvatochromism of compound 3 in different solvents. (Bottom) Charge-transfer bands of compound 3 in 17 different solvents.

tion and recombination resulting from the internal bond length alterations (or vibrational changes),  $\lambda_v$ , and the outer solvent reorganizations,  $\lambda_o$ . For asymmetric compounds, an additional term,  $\Delta G^\circ$ , named redox or energetic asymmetry, describing the energy difference between the charge-separated  $D^+A^-$  state and the neutral DA ground state is added, so that the total energy balance is expressed as follows:<sup>29</sup>

$$E_{\text{opt}} = h\nu_{\text{max}} = \lambda_v + \lambda_o + \Delta G^\circ \quad (1)$$

The solvent dependence of the optical energy of the CT band enters into this formula in two different ways: one is by the outer solvent reorganization energy, but it also plays a role through the redox asymmetry term, while the internal (vibrational) reorganization energy is supposed not to vary with the solvent.<sup>30</sup> In this part, the solvent dependence of spectroscopic data of our set of 2-amino-naphtho[2,3-*b*]furan-4,9-dione derivatives (1–8) is described. This will corroborate the cyclic voltammetry results in terms of the electron delocalization. Moreover, it will describe the interactions of such compounds with their surrounding media, an important factor for their cytotoxic activity.

All compounds exhibit a broad absorption band in the visible region of their spectra that presents an intense solvatochromism ( $\Delta\lambda \approx 80$  nm) going from orange to blue when moving from hexane to ethanol (Figure 9 and Table S1 in Supporting Information).

These bands correspond to the excitation of a neutral DA ground state to the charge separated state  $D^+A^-$ , indicative of an intramolecular electron transfer process of amino-substituted quinonoid  $\pi-\pi^*$  structures.<sup>31</sup> Looking how the  $\nu_3$  ( $\text{cm}^{-1}$ ) of the IET band varies with the solvent polarity measured by their relative permittivity ( $\epsilon_r$ ) (Figure 10), a clear deviation from linearity is detected. Therefore, it is corroborated that the solvent cannot be considered as a structureless continuum and that specific solvent/solute interactions must be playing an important role. To take into account such specific interactions and explain in more detail the solvatochromic behavior that these compounds exhibit, a linear solvation energy relationship was used.

The LSER treatment is a powerful tool for the study of the principal intermolecular interactions that control a specific

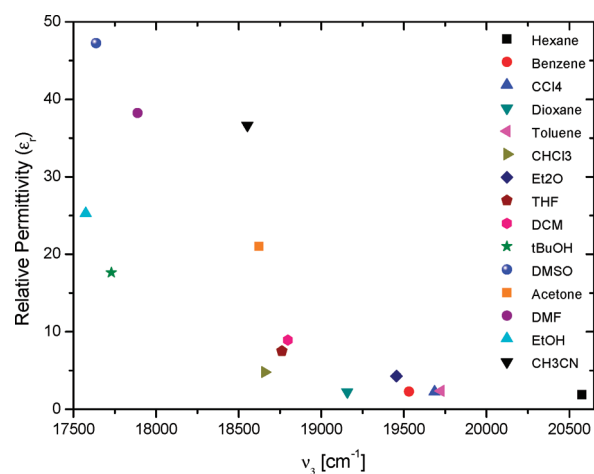


**Figure 10.** Relationship between the observed IET band  $\nu_3$  ( $\text{cm}^{-1}$ ) for compound 3 and the relative permittivity  $\epsilon_r$  of the solvents.

physicochemical process in solution. The LSER assumes that the changes in the free energy associated with a physicochemical process are the sum of different independent contributions generated from the different solute/solvent interactions. In this case, it was confirmed that there are three parameters to be considered:  $\alpha$ ,  $\beta$ , and  $\pi^*$ .<sup>28</sup> The nonspecific parameter  $\pi^*$  measures the attractive effect of dipole/dipole and dipole/induced dipole interactions between the solute and the solvent molecules, i.e., it is a measure of the dipolarity/polarizability. The solvatochromic specific parameter  $\beta$  is a quantitative empirical measure of the ability of a solvent to act as hydrogen-bond acceptor (HBA)<sup>15</sup> or electron donor toward a standard solute, i.e., it is a measure of the basicity of the solvent. By contrast, the specific empirical parameter  $\alpha$  quantitatively measures the ability of a solvent to act as a hydrogen-bond donor (HBD)<sup>15</sup> or electron-pair acceptor toward a standard solute, i.e., it is a measure of the acidity of the solvent.<sup>29</sup> Therefore, the generalized LSER equation that describes the IET energy associated with the

**Table 4.** LSER Values Obtained by a Multivariable Linear Regression Fit for Compound 3<sup>a</sup>

	coeff	std error	std coeff	tolerance	<i>t</i>	<i>p</i>
$\nu_i^\circ$	20.543	0.056	0		365.938	<0.0004
$a_3$	-1.064	0.126	-0.272	0.721	-8.446	<0.0004
$b_3$	-1.679	0.106	-0.541	0.647	-15.915	<0.0004
$s_3$	-1.602	0.087	-0.547	0.847	-18.402	<0.0004

<sup>a</sup>Standardized coefficients and distribution values (*t*) indicate the goodness of this method (*p*); whereas the tolerance is an indication of the orthogonality among  $a_3$ ,  $b_3$ , and  $s_3$ .  $R = 0.995$ . Standard error of estimate = 0.095

CT absorption for a donor–acceptor dyad in any solvent media adopts the form of eq 2:

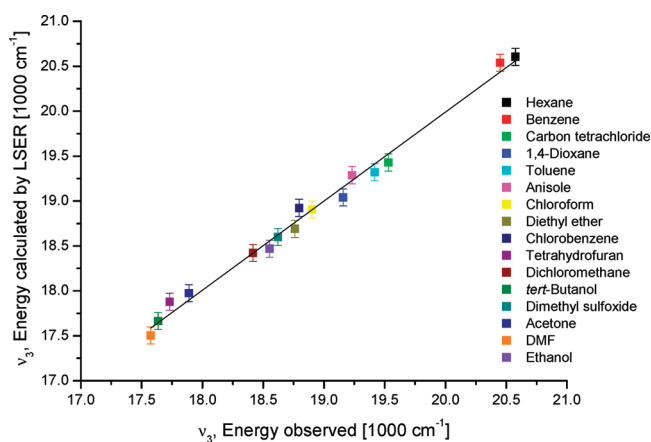
$$\nu_i = \nu_i^\circ + a_i\alpha + b_i\beta + s_i\pi^* \quad (2)$$

where the coefficients  $a_i$ ,  $b_i$ ,  $s_i$ , and the constant  $\nu_i^\circ$  are characteristic of each studied compound *i* independent of the nature of the solvent. These coefficients are indicative of the sensitivity of the IET process exhibited by the compound *i* toward the variation of each solvent property ( $\alpha$ ,  $\beta$ , and  $\pi^*$ ). Such coefficients must have negative (or positive) signs according to the nature of each term, and the independent term  $\nu_i^\circ$  (in  $\text{cm}^{-1}$ ) is the energy of the absorption expected for the IET process in the absence of a solvent, i.e., in a vacuum.<sup>29</sup> The energies of the CT bands were measured for compound 3 at room temperature in 17 different solvents, which were chosen as representative of the 11 groups in which the most common laboratory solvents are classified.<sup>32</sup> By fitting the experimental data  $\nu_3$  ( $\text{cm}^{-1}$ ) obtained in different solvents with the known  $\alpha$ ,  $\beta$ , and  $\pi^*$  parameters for each solvent to the eq 2 through a multivariable linear regression, the coefficients  $a_i$ ,  $b_i$ ,  $s_i$  and the independent term  $\nu_i^\circ$ , corresponding to the IET process were calculated for compound 3. By means of statistical analysis, those coefficients with a low significance level were removed from the calculated model. The LSER treatment of the experimental spectroscopic data of compound 3 demonstrates the presence of specific H-bonding interactions between this compound and the solvent along with nonspecific dipolarity/polarizability interactions that contribute significantly to the solvent-induced IET process. The final LSER model obtained is described in Table 4 and summarized by eq 3:

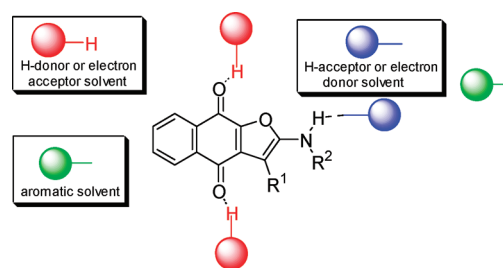
$$\nu_3 = 20.543(\pm 0.056) - 1.064(\pm 0.126)\alpha - 1.679(\pm 0.106)\beta - 1.602(\pm 0.087)\pi^* \quad (3)$$

Figure 11 shows the good agreement achieved between the calculated IET energy from the LSER model obtained for each solvent and the experimental data for compound 3.

From the analysis of the LSER model, the following information can be extracted: (a) The IET energy for compound 3 is very sensitive to changes of the HBD or HBA abilities of the surrounding media. Thus, the negative values obtained for the coefficients  $a_3$  and  $b_3$  result in a decrease in the energy (red shift) of the IET band with increasing solvent hydrogen-bond donor ( $\alpha$ ) or acceptor abilities ( $\beta$ ). The decrease of energy with the increasing of  $\alpha$  can be explained in terms of the quinone structure due to the capability of its carbonyl groups to interact with HBD solvents. Similarly, the HBA solvents are able to interact with the 2-amino-naphtho[2,3-*b*]furan-4,9-dione derivatives through their amino function (Figure 12) leading to a decrease in energy when  $\beta$  increases. Therefore, it can be concluded that the



**Figure 11.** IET energies, calculated using the LSER eq 3, versus the experimentally observed values.



**Figure 12.** Scheme of different solvent interactions with the 2-amino-naphtho[2,3-*b*]furan-4,9-dione derivatives.

hydrogen-bond formation between these compounds and the solvent enhances the stability of the whole system. (b) The excited state of 3 and the corresponding ones for the other compounds 1–8 present larger dipole moments and greater polarizabilities than the corresponding electronic ground states. Since the  $\pi^*$  values measure the dipolarity/polarizability of the solvents, the negative sign of  $s_3$  indicates a greater stabilization of the excited state by means of larger dipole/dipole and dispersion interactions with increasing  $\pi^*$  values, as compared to the electronic ground state.

To determine the solvent effect on the IET band of the rest of our family of 2-amino-naphtho[2,3-*b*]furan-4,9-diones, derivatives 1–8 were studied. Taking into account the important specific and nonspecific parameters  $\alpha$ ,  $\beta$ , and  $\pi^*$ , three representative solvents were selected to describe the solvent influence on the IET of these 2-amino-naphtho[2,3-*b*]furan-4,9-diones: toluene as a nonpolar one, acetonitrile as a polar one, and ethanol as polar and protic one.

The following spectroscopic data were obtained for each compound (Table 5): (a) In general terms, the solvent tendency previously described for compound 3 is maintained in each derivative. Therefore, an increase of any parameter  $\alpha$ ,  $\beta$ , or  $\pi^*$  causes a decrease in the energy and a red shift of the IET band, which can be explained as an increase of the stability of these molecules in the surrounding media. (b) Derivatives substituted with aromatic functions like 5, 6, 7, and 8 present less solvatochromism, which is indicative of being more stable than the other ones due to their capability of delocalizing their electrons and stabilizing the charge separated state as it was observed in the cyclic voltammetry experiments. Moreover, those compounds that contain aromatic groups at the C-3 of the furan ring (5 and

**Table 5.** Solvatochromism of the IET Band of Several 2-Amino-naphtho[2,3-*b*]furan-4,9-dione Derivatives in Toluene (tol), Acetonitrile (AN), and Ethanol (OH)

	$\lambda_{\text{tol}}^a$ (nm)	$\lambda_{\text{AN}}^a$ (nm)	$\lambda_{\text{OH}}^a$ (nm)	$\varepsilon_{\text{tol}}^b$ (cm <sup>-1</sup> M <sup>-1</sup> )	$\varepsilon_{\text{AN}}^b$ (cm <sup>-1</sup> M <sup>-1</sup> )	$\varepsilon_{\text{OH}}^b$ (cm <sup>-1</sup> M <sup>-1</sup> )	$\Delta\lambda_{\text{tol/OH}}^c$ (nm)
1	521	550	577	4780	5744	7605	56
2	523	553	580	4076	5184	7327	57
3	508	541	568	4033	4714	4903	60
4	511	542	569	4170	5331	6700	58
5	524	541	556	5427	5784	6230	32
6	531	549	568	4908	5407	6162	37
7	514	538	565	4263	4834	5259	51
8	509	538	564	1475	1708	2443	55

<sup>a</sup>  $\lambda_{\text{max}}$  of a given compound in solvent *i*. <sup>b</sup>  $\varepsilon_{\text{max}}$  of a given compound in solvent *i*. <sup>c</sup>  $\Delta\lambda_{i/j} = \lambda_{\text{max},j} - \lambda_{\text{max},i}$  being *i*, *j* solvents.

6) are even more stable than those that have aromatic functions in the amino position (7 and 8) due to their capability of a better delocalization of their electrons through the quinoid structure. (c) The dependence of the solvent polarity with the molar absorption coefficients presents the same tendency. Therefore, the highest  $\varepsilon$  values were obtained in ethanol according to other systems previously described in the literature.<sup>29</sup>

## CONCLUSIONS

In this paper we present a new set of cytotoxic 2-amino-naphtho[2,3-*b*]furan-4,9-dione derivatives (1–8). A relationship between the electronic properties of these compounds and their cytotoxicity against several human tumor cell lines (MCF7, MCF7/BUS, and SK-Br-3) is established: the more delocalized the electronic system, the greater the cytotoxic activity. The electron delocalization is quantitatively evaluated by means of reduction potentials and, in a more novel approach, by the solvatochromism of the IET band through a LSER treatment. Hence, high electron delocalizations imply high redox potentials and small solvatochromic effects. In fact, we can affirm that compounds with  $E_{(1/2)}^1 > -1,250$  V and  $\Delta\lambda_{\text{tol/OH}} < 40$  nm are extremely susceptible to present cytotoxic activity against the studied tumor cell lines. This observed trend can be easily explained taking into account the reduction potential. Thus, a high reduction potential facilitates semiquinone formation and therefore the bioreduction step that is supposed to initiate the cytotoxic activity of such compounds. Moreover, an influence of the atmospheric oxygen is demonstrated that suggests that the mechanism of action of our compounds involves reactive oxygen species. Moreover, the LSER treatment allowed the determination of the principal interactions that these compounds 1–8 present with their surrounding media, the capacity of acting as electron donors and acceptors and the dipolarity/polarizability being the most important. These interactions not only play a role from the electronic point of view but also from the structural one.

## EXPERIMENTAL SECTION

**General Methods.** All solvents and reagents were purified by standard techniques reported (Perrin, D. D.; Amarego, W. L. F. In *Purification of Laboratory Chemicals*, 3rd ed.; Pergamon: Oxford, 1988) or used as supplied from commercial sources when appropriate. Reactions were monitored by TLC (on silica gel POLYGRAM SIL G/UV254 foils). Precoated TLC plates SIL G-100 UV254 were used for preparative TLC purification. <sup>1</sup>H NMR spectra were recorded in CDCl<sub>3</sub> at 300 and 400 MHz. All compounds were named using ACD40 Name-Pro program, which is based on IUPAC rules. Cyclic voltammetry experiments were performed

using Pt as working and counter electrodes. The reference electrode was Ag/AgCl. However, the potential values obtained are referred to Fc/Fc<sup>+</sup> as recommended by IUPAC. The concentrations of the samples were 1 mM in DMF using tetrabutylammonium hexafluorophosphate (HFPTBA) as supporting electrolyte (0.1 M). Different scan rates (50–125 mV s<sup>-1</sup>) were used. All studies were carried out in an inert atmosphere by saturation with argon during several minutes at room temperature. Each absorption spectrum reported is the median of 3 spectra whose extinction coefficients did not differ significantly. Each spectrum was obtained from an independent solution of the corresponding studied compound. The spectra were performed at room temperature.

**General Procedure for the Synthesis of 2-Amino-naphtho[2,3-*b*]furan-4,9-dione Derivatives.** The synthesis of 2-amino-naphtho[2,3-*b*]furan-4,9-dione derivatives was made following a modified methodology described by Teimouri, et al.<sup>18</sup> 2-Hydroxy-1,4-naphthoquinone (100.0 mg, 0.547 mmol) in 10 mL of toluene was treated with 1.2 equiv of aldehyde, 1.2 equiv of isocyanide, and catalytic amounts of EDDA (ethylenediamino diacetate, 5% mmol). The reaction mixture was heated under reflux and checked by TLC until disappearance of the starting naphthoquinone. Then, the reaction mixture was cooled, and the toluene was removed under reduced pressure. The crude was purified by silica gel column chromatography with Hex/EtOAc as a mixture of solvents.

**2-Cyclohexylamino-3-ethylnaphtho[2,3-*b*]furan-4,9-dione (1).** Following the general procedure described above, 100.0 mg (0.574 mmol) of 2-hydroxy-1,4-naphthoquinone in 10 mL of toluene was treated with 1.2 equiv of propionaldehyde (0.689 mmol, 0.049 mL), 1.2 equiv of cyclohexyl isocyanide (0.689 mmol, 0.085 mL), and 0.1 equiv of EDDA (0.057 mmol, 10.3 mg). The reaction mixture was refluxed for 30 min. The solvent was removed under vacuum, and the crude was purified by flash chromatography (silica gel, Hex/EtOAc 9:1) to provide 1 (144.3 mg, 77%) as an amorphous blue solid. IR (neat)  $\nu_{\text{max}}$  2931, 2856, 1642, 1587, 1540, 1489, 1453, 1350, 1285, 1257, 1220, 1153, 1114, 1082, 1030, 996, 966, 891, 847, 812, 755, 698 cm<sup>-1</sup>; <sup>1</sup>H NMR (300 MHz; CDCl<sub>3</sub>)  $\delta$  1.11 (3 H, t, *J* = 7.4 Hz), 1.18–1.42 (5 H, m), 1.60 (1 H, m), 1.71 (2 H, m), 2.02 (2 H, m), 2.59 (2 H, m), 3.74 (1 H, m), 4.84 (1 H, d, *J* = 8.2 Hz), 7.53 (1 H, t, *J* = 7.3 Hz), 7.62 (1 H, t, *J* = 7.3 Hz), 7.99 (1 H, d, *J* = 7.3 Hz), 8.09 (1 H, d, *J* = 7.4 Hz); <sup>13</sup>C NMR (75 MHz; CDCl<sub>3</sub>)  $\delta$  13.6 (CH<sub>3</sub>), 15.5 (CH<sub>2</sub>), 24.5 (2 × CH<sub>2</sub>), 25.1 (CH<sub>2</sub>), 33.7 (2 × CH<sub>2</sub>), 52.2 (CH), 101.0 (C), 125.7 (CH), 125.8 (CH), 131.5 (CH), 132.4 (C), 132.6 (C), 133.4 (CH), 133.7 (C), 142.0 (C), 159.3 (C), 167.6 (C), 182.8 (C); EIMS *m/z* 323 [M<sup>+</sup>] (43), 241 (100), 226 (39), 55 (15); HREIMS 323.1521 (calcd for C<sub>20</sub>H<sub>21</sub>NO<sub>3</sub>, 323.1516).

**2-Cyclohexylamino-3-hexyl-naphtho[2,3-*b*]furan-4,9-dione (2).** Following the general procedure described above 100.0 mg of 2-hydroxy-1,4-naphthoquinone (0.574 mmol) in toluene (10 mL) was treated with 1.2 equiv of heptaldehyde (0.689 mmol, 0.096 mL), 1.2 equiv of cyclohexyl isocyanide (0.689 mmol, 0.085 mL), and 0.1 equiv of EDDA (0.057 mmol, 10.3 mg). The mixture was heated under reflux for 30 min under nitrogen atmosphere. Then, the solution was cooled at room temperature, and the



solvent was removed under reduced pressure. The crude was purified by flash chromatography (silica gel, Hex/EtOAc 9:1) to provide **2** (205.4 mg, 94%) as an amorphous blue solid. IR (neat)  $\nu_{\max}$  2926, 1725, 1662, 1641, 1587, 1537, 1465, 1447, 1085, 875  $\text{cm}^{-1}$ ;  $^1\text{H NMR}$  (300 MHz;  $\text{CDCl}_3$ )  $\delta$  0.80 (3 H, s), 1.23–1.30 (8 H, m), 1.40–1.45 (2 H, m), 1.53 (2 H, m), 1.64 (2 H, m), 1.76 (2 H, m), 2.25 (2 H, m), 2.55 (2 H, t,  $J = 7.4$  Hz), 3.79 (1 H, m), 4.33 (1 H, d,  $J = 7.8$  Hz), 7.70 (1 H, t,  $J = 7.2$  Hz), 7.77 (1 H, t,  $J = 7.1$  Hz), 8.12 (1 H, d,  $J = 7.2$  Hz), 8.16 (1 H, d,  $J = 7.3$  Hz);  $^{13}\text{C NMR}$  (75 MHz;  $\text{CDCl}_3$ )  $\delta$  13.8 (c), 22.2 (t), 22.4 (t), 24.5 (2t), 25.1 (t), 28.8 (t), 29.1 (t), 31.4 (t), 33.8 (2t), 52.1 (d), 99.5 (s), 125.8 (d  $\times$  2), 131.5 (d), 132.5 (s), 132.7 (s), 133.4 (d), 133.6 (s), 142.4 (s), 159.3 (s), 168.1 (s), 182.5 (s);  $m/z$  (EI): 379 ( $\text{M}^+$ , 100), 308 (20), 297 (31), 226 (80), 55 (21); HREIMS 379.2147 (calcd for  $\text{C}_{24}\text{H}_{29}\text{NO}_3$ , 379.2129).

**2-tert-Butylamino-3-ethyl-naphtho[2,3-b]furan-4,9-dione (3).** Following the general procedure described above, 100.0 mg (0.574 mmol) of 2-hydroxy-1,4-naphthoquinone in 10 mL of toluene was treated with 1.2 equiv of propionaldehyde (0.689 mmol, 0.049 mL), 1.2 equiv of *tert*-butyl isocyanide (0.689 mmol, 0.078 mL), and 0.1 equiv of EDDA (0.057 mmol, 10.3 mg). The mixture was refluxed for 30 min under nitrogen atmosphere. Then, the solution was cooled to room temperature, and the solvent was removed under reduced pressure. The crude was purified by flash chromatography (silica gel, Hex/EtOAc 9:1) to provide **3** (154.3 mg, 90%) as an amorphous blue solid. IR (neat)  $\nu_{\max}$  2930, 1709, 1641, 1584, 1538, 1464, 1369, 1281, 1207, 1083, 874, 755, 702  $\text{cm}^{-1}$ ;  $^1\text{H NMR}$  (300 MHz;  $\text{CDCl}_3$ )  $\delta$  1.10 (3 H, t,  $J = 7.5$  Hz), 1.42 (9 H, s), 2.57 (2 H, c), 4.74 (1 H, s), 7.53 (1 H, t,  $J = 7.4$  Hz), 7.59 (1 H, t,  $J = 7.4$  Hz), 7.96 (1 H, d,  $J = 7.5$  Hz), 8.07 (1 H, d,  $J = 7.5$  Hz);  $^{13}\text{C NMR}$  (75 MHz;  $\text{CDCl}_3$ )  $\delta$  13.6 (3  $\times$   $\text{CH}_3$ ), 15.7 ( $\text{CH}_2$ ), 29.8 ( $\text{CH}_3$ ), 53.6 (C), 103.3 (C), 125.7 (CH), 125.8 (CH), 131.5 (C), 131.6 (CH), 132.6 (C), 133.3 (CH), 133.5 (C), 143.1 (C), 159.3 (C), 168.1 (C), 182.6 (C); EIMS  $m/z$  297 [ $\text{M}^+$ ] (15), 241 (100), 55 (12); HREIMS 297.1365 (calcd for  $\text{C}_{18}\text{H}_{19}\text{NO}_3$ , 297.1357).

**2-tert-Butylamino-3-ethyl-naphtho[2,3-b]furan-4,9-dione (4).** 2-Hydroxy-1,4-naphthoquinone (100.0 mg, 0.574 mmol) in 10 mL of toluene was treated with 1.2 equiv of heptaldehyde (0.689 mmol, 0.096 mL), 1.2 equiv of *tert*-butyl isocyanide (0.689 mmol, 0.078 mL), and 0.1 equiv of EDDA (0.057 mmol, 10.3 mg). The reaction mixture was refluxed for 30 min under nitrogen atmosphere. The solvent was removed under vacuum, and the crude was purified by flash chromatography (silica gel, Hex/EtOAc 9:1) to provide **4** (159.4 mg, 79%) as an amorphous blue solid. IR (neat)  $\nu_{\max}$  2859, 1641, 1583, 1539, 1463, 1369, 1273, 1258, 1083, 933, 756  $\text{cm}^{-1}$ ;  $^1\text{H NMR}$  (300 MHz;  $\text{CDCl}_3$ )  $\delta$  0.77 (3 H, s), 1.20 (6 H, m), 1.42 (6 H, s), 1.47 (5 H, m), 2.53 (2 H, t,  $J = 7.4$  Hz), 4.82 (1 H, s), 7.53 (1 H, t,  $J = 7.4$  Hz), 7.59 (1 H, t,  $J = 7.4$  Hz), 7.96 (1 H, d,  $J = 7.5$  Hz), 8.06 (1 H, d,  $J = 7.5$  Hz);  $^{13}\text{C NMR}$  (75 MHz;  $\text{CDCl}_3$ )  $\delta$  13.17 ( $\text{CH}_3$ ), 22.3 (2  $\times$   $\text{CH}_2$ ), 28.8 ( $\text{CH}_2$ ), 29.1 ( $\text{CH}_2$ ), 29.8 ( $\text{CH}_3 \times 3$ ), 31.4 ( $\text{CH}_2$ ), 53.5 (C), 101.8 (C), 125.7 (CH), 125.8 (CH), 131.5 (CH), 131.7 (C), 132.7 (C), 133.3 (CH), 133.5 (C), 143.0 (C), 159.7 (C), 167.9 (C), 182.6 (C); EIMS  $m/z$  353 [ $\text{M}^+$ ] (24), 297 (96), 226 (100); HREIMS 353.1991 (calcd for  $\text{C}_{22}\text{H}_{27}\text{NO}_3$ , 353.1996).

**2-tert-Butylamino-3-phenyl-naphtho[2,3-b]furan-4,9-dione (5).** Following the general procedure described above, 100.0 mg (0.574 mmol) of 2-hydroxy-1,4-naphthoquinone in 10 mL of toluene was treated with 1.2 equiv of benzaldehyde (0.689 mmol, 0.070 mL), 1.2 equiv of *tert*-butyl isocyanide (0.689 mmol, 0.078 mL), and 0.1 equiv of EDDA (0.057 mmol, 10.3 mg). The reaction mixture was refluxed for 30 min under nitrogen atmosphere. The solvent was removed under vacuum, and the crude was purified by flash chromatography (silica gel, Hex/EtOAc 9:1) to provide **5** (114.2 mg, 57%) as an amorphous blue solid. IR (neat)  $\nu_{\max}$  2971, 1709, 1671, 1640, 1580, 1538, 1508, 1460, 1345, 1250, 1202, 1169, 1083, 973, 918, 805, 752, 696  $\text{cm}^{-1}$ ;  $^1\text{H NMR}$  (300 MHz;  $\text{CDCl}_3$ )  $\delta$  1.48 (9 H, s), 5.02 (1 H, m), 7.31 (1 H, m), 7.39 (4 H, m), 7.46 (1 H, t,  $J = 6.5$ ), 7.58 (1 H, t,  $J = 6.4$  Hz), 7.98 (1 H, d,  $J = 7.4$  Hz), 8.11 (1 H, d,  $J = 7.5$  Hz);  $^{13}\text{C NMR}$  (75 MHz;  $\text{CDCl}_3$ )  $\delta$  29.7 (3  $\times$   $\text{CH}_3$ ), 53.7 (C), 100.0 (C), 125.7 (CH), 126.1 (CH), 127.4 (CH), 128.5 (CH  $\times$  2), 129.1 (CH  $\times$  2), 129.9 (C), 130.1 (C), 131.9

(CH), 132.9 (C), 133.0 (C), 133.3 (CH), 143.6 (C), 159.2 (C), 168.9 (C), 181.4 (C); EIMS  $m/z$  345 [ $\text{M}^+$ ] (17), 289 (100), 272 (8), 233 (10), 204 (7); HREIMS 345.1365 (calcd for  $\text{C}_{22}\text{H}_{19}\text{NO}_3$ , 345.1376).

**2-tert-Butylamino-3-furan-3-yl-naphtho[2,3-b]furan-4,9-dione (6).** Following the general procedure described above, 100.0 mg (0.574 mmol) of 2-hydroxy-1,4-naphthoquinone in 10 mL of toluene was treated with 1.2 equiv of 3-furaldehyde (0.689 mmol, 0.060 mL), 1.2 equiv of *tert*-butyl isocyanide (0.689 mmol, 0.078 mL), and 0.1 equiv of EDDA (0.057 mmol, 10.3 mg). The reaction mixture was refluxed for 30 min under nitrogen atmosphere. The solvent was removed under vacuum, and the crude was purified by flash chromatography (silica gel, Hex/EtOAc 9:1) to provide **6** 185.6 mg (96%) as an amorphous blue solid. IR (neat)  $\nu_{\max}$  2974, 1647, 1595, 1541, 1458, 1370, 1260, 1204, 1160, 1099, 1048, 995, 935, 908, 871, 790, 756, 727, 696, 644  $\text{cm}^{-1}$ ;  $^1\text{H NMR}$  (300 MHz;  $\text{CDCl}_3$ )  $\delta$  1.51 (9H, s), 4.87 (1H, s), 6.73 (1H, s), 7.53 (1H, s), 7.59 (1H, t,  $J = 7.4$  Hz), 7.67 (1H, t,  $J = 7.4$  Hz), 7.82 (1H, s), 8.03 (1H, d,  $J = 7.4$  Hz), 8.13 (1H, d,  $J = 7.5$  Hz);  $^{13}\text{C NMR}$  (75 MHz;  $\text{CDCl}_3$ )  $\delta$  29.7 ( $\text{CH}_3 \times 3$ ), 53.8 (C), 91.5 (C), 110.4 (CH), 114.5 (C), 125.7 (CH), 126.1 (CH), 130.0 (C), 131.9 (CH), 132.8 (C), 133.0 (C), 133.4 (CH), 140.7 (CH), 143.0 (CH), 143.7 (C), 159.0 (C), 168.9 (C), 181.6 (C); EIMS  $m/z$  335 [ $\text{M}^+$ ] (20), 279 (100), 251 (18), 223 (12), 139 (88); HREIMS 335.1158 (calcd for  $\text{C}_{20}\text{H}_{17}\text{NO}_4$ , 335.1161).

**2-Benzylamino-3-ethyl-naphtho[2,3-b]furan-4,9-dione (7).** 2-Hydroxy-1,4-naphthoquinone (100.0 mg, 0.574 mmol) in 10 mL of toluene was treated with 1.2 equiv of propionaldehyde (0.689 mmol, 0.5 mL), 1.2 equiv of benzyl isocyanide (0.689 mmol, 0.078 mL), and 0.1 equiv of EDDA (0.057 mmol, 10.3 mg). The reaction mixture was refluxed for 30 min under nitrogen atmosphere. The solvent was removed under vacuum, and the crude was purified by flash chromatography (silica gel, Hex/EtOAc 9:1) to provide **7** (170.1 mg, 89%) as an amorphous blue solid. IR (neat)  $\nu_{\max}$  1709, 1643, 1591, 1543, 1493, 1450, 1354, 1285, 1220, 1126, 1083, 1026, 994, 961, 754, 697  $\text{cm}^{-1}$ ;  $^1\text{H NMR}$  (300 MHz;  $\text{CDCl}_3$ )  $\delta$  1.16 (3 H, t,  $J = 7.4$  Hz), 2.63 (2 H, c), 4.62 (2 H, d,  $J = 5.9$  Hz), 5.19 (1 H, t,  $J = 5.3$  Hz), 7.26–7.31 (5 H, m), 7.57 (1 H, t,  $J = 7.2$  Hz), 7.64 (1 H, t,  $J = 7.3$  Hz), 8.01 (1 H, d,  $J = 7.4$  Hz), 8.09 (1 H, d,  $J = 7.4$  Hz);  $^{13}\text{C NMR}$  (75 MHz;  $\text{CDCl}_3$ )  $\delta$  13.7 ( $\text{CH}_3$ ), 15.6 ( $\text{CH}_2$ ), 47.3 ( $\text{CH}_2$ ), 100.8 (C), 125.8 (CH), 125.9 (CH), 127.5 (2  $\times$  CH), 127.7 (CH), 128.3 (C), 128.6 (CH  $\times$  2), 131.7 (CH), 132.3 (C), 132.7 (C), 133.4 (CH), 137.3 (C), 142.5 (C), 158.9 (C), 168.5 (C), 182.7 (C); EIMS  $m/z$  331 [ $\text{M}^+$ ] (45), 240 (10), 213 (8), 91 (100); HREIMS 331.1208 (calcd for  $\text{C}_{21}\text{H}_{17}\text{NO}_3$ , 331.1211).

**2-Benzylamino-3-cyclohexyl-naphtho[2,3-b]furan-4,9-dione (8).** Following the general procedure described above, 100.0 mg (0.574 mmol) of 2-hydroxy-1,4-naphthoquinone in 10 mL of toluene was treated with 1.2 equiv of cyclohexanecarbaldehyde (0.689 mmol, 0.083 mL), 1.2 equiv of benzyl isocyanide (0.689 mmol, 0.084 mL), and 0.1 equiv of EDDA (0.057 mmol, 10.3 mg). The reaction mixture was refluxed for 30 min under nitrogen atmosphere. The solvent was removed under vacuum, and the crude was purified by flash chromatography (silica gel, Hex/EtOAc 9:1) to provide **8** (216.5 mg, 97%) as an amorphous blue solid. IR (neat)  $\nu_{\max}$  2925, 2853, 1725, 1641, 1587, 1534, 1447, 1345, 1212, 1083, 874, 789, 754, 698  $\text{cm}^{-1}$ ;  $^1\text{H NMR}$  (300 MHz;  $\text{CDCl}_3$ )  $\delta$  1.20–1.28 (2 H, m), 1.65–1.76 (8 H, m), 1.98 (1 H, m), 4.05 (2 H, s), 5.69 (1 H, s), 7.14–7.25 (5 H, m), 7.59 (1 H, t,  $J = 7.4$  Hz), 7.65 (1 H, t,  $J = 7.2$  Hz), 8.04 (1 H, d,  $J = 7.1$  Hz), 8.11 (1 H, d,  $J = 7.2$  Hz);  $^{13}\text{C NMR}$  (75 MHz;  $\text{CDCl}_3$ )  $\delta$  25.4 ( $\text{CH}_3$ ), 26.5 (2  $\times$   $\text{CH}_2$ ), 30.75 (2  $\times$   $\text{CH}_2$ ), 33.58 (CH), 47.1 ( $\text{CH}_2$ ), 104.7 (C), 125.5 (CH), 126.0 (CH), 127.3 (CH  $\times$  2), 127.4 (CH), 128.4 (2  $\times$  CH), 131.7 (CH), 132.4 (C), 132.8 (C), 133.1 (C), 133.3 (CH), 137.5 (C), 142.7 (C), 158.9 (C), 168.3 (C), 182.3 (C); EIMS  $m/z$  385 ( $\text{M}^+$ , 67), 91 (100); HREIMS 385.1678 (calcd for  $\text{C}_{25}\text{H}_{23}\text{NO}_3$ , 385.1675).

**Biological Assays.** All starting materials were commercially available research-grade chemicals and were used without further purification. RPMI 1640 medium was purchased from Flow Laboratories (Irvine, U.K.), fetal calf serum (FCS) was from Gibco (Grand Island, NY), trichloroacetic acid (TCA) and glutamine were from Merck (Darmstadt, Germany), and



penicillin G, streptomycin, dimethyl sulfoxide (DMSO), and sulforhodamine B (SRB) were from Sigma (St. Louis, MO).

**Cells, Culture, and Plating.** The human solid tumor cell lines MCF-7 and SK-Br-3 were obtained from the American Type Culture Collection (ATCC, Rockville, MD), and MCF-7BUS cells were kindly provided by Dr. Nicolás Olea Serrano from the University of Granada (Spain). Cells were maintained in 25 cm<sup>2</sup> culture flasks in RPMI 1640 medium supplemented with 5% heat-inactivated fetal calf serum and 2 mM L-glutamine in a 37 °C, 5% CO<sub>2</sub>, 95% humidified air incubator. Exponentially growing cells were trypsinized and resuspended in antibiotic-containing medium (100 units penicillin G and 0.1 mg of streptomycin per mL). Single cell suspensions displaying >97% viability by trypan blue dye exclusion were subsequently counted. After counting, dilutions were made to give the appropriate cell densities for inoculation onto 96-well microtiter plates. Cells were inoculated in a volume of 100 μL per well at densities of 12,000 (MCF-7 and MCF-7/BUS) and 15,000 (SK-Br-3) cells per well, based on their doubling times.

**Chemosensitivity Testing.** Chemosensitivity tests were performed using the SRB assay of the U.S. NCI with slight modifications. Briefly, pure compounds were initially dissolved in DMSO at 400 times the desired final maximum test concentration. Control cells were exposed to an equivalent concentration of DMSO (0.25% v/v, negative control). Each agent was tested in triplicate at different dilutions in the range 1–100 μM. The test compound treatment was started on day 1 after plating. Drug incubation times were 48 h, after which time cells were precipitated with 25 μL of ice-cold 50% (w/v) trichloroacetic acid and fixed for 60 min at 4 °C. Then, the SRB assay was performed. The optical density (OD) of each well was measured at 492 nm, using a PowerWave XS Absorbance microplate reader (BioTek). Values were corrected for background OD from wells containing only medium. The percentage growth (PG) was calculated with respect to untreated control cells (C) at each of the drug concentration levels based on the difference in OD at the start (T<sub>0</sub>) and end of drug exposure (T), according to the NCI protocol. Therefore, if T was greater than or equal to T<sub>0</sub> the calculation was  $100 \times [(T - T_0)/(C - T_0)]$ . If T was less than T<sub>0</sub>, denoting cell death, the calculation was  $100 \times [(T - T_0)/T_0]$ . The effect was defined as percentage of growth, where 50% growth inhibition (GI50), total growth inhibition (TGI), and 50% cell killing (LC50) represent the concentration at which PG is +50, 0, and -50, respectively. With these calculations, a PG value of 0 corresponded to the amount of cells present at the start of drug exposure, while negative PG values denoted net cell kill.

## ■ ASSOCIATED CONTENT

Supporting Information. <sup>1</sup>H NMR and <sup>13</sup>C NMR spectra of compounds 1–8, crystallographic data of compound 3 in CIF format, and spectral data for the IET band of 3 in different solvents. This material is available free of charge via the Internet at <http://pubs.acs.org>.

## ■ AUTHOR INFORMATION

### Corresponding Author

\*E-mail: [agravelo@ull.es](mailto:agravelo@ull.es); [vecianaj@icmab.es](mailto:vecianaj@icmab.es); [aestebra@ull.es](mailto:aestebra@ull.es).

## ■ ACKNOWLEDGMENT

We gratefully acknowledge the financial support from MICINN-Spain Projects “Eje C-Consolider” CTQ2006-06333/BQU and CTQ2010-19501, SAF 2009-13296-CO2-01, AGAUR grant 2009SGR-00516 from Generalitat de Catalunya, CIBER de Bioingeniería, Biomateriales y Nanomedicina (CIBER-BBN is an initiative funded by the VI National R&D&I Plan 2008-2011,

Iniciativa Ingenio 2010, Consolider Program, CIBER Actions and financed by the Instituto de Salud Carlos III with assistance from the European Regional Development Fund). J.G. thanks CSIC for a predoctoral grant. J.G. realized part of this work in the framework of the “Material Science PhD Program” of the Autonomous University of Barcelona (UAB). S.J.-A. thanks MICINN-Spain for a predoctoral grant. We also thank CEAMED (Dr. Rubén Pérez-Machín) for carrying out the cytotoxic assays and the ICIC for financial support.

## ■ REFERENCES

- (1) Hui, Y.; Khim Chng, E. L.; Lin Chng, C. Y.; Poh, H. L.; Webster, R. D. *J. Am. Chem. Soc.* **2009**, *131*, 1523–1534.
- (2) Ogawa, M.; Koyanagi, J.; Sugaya, A.; Tsuda, T.; Ohguchi, H.; Nakayama, K.; Yamamoto, K.; Tanaka, A. *Biosci. Biotechnol. Biochem.* **2006**, *70*, 1009–1012.
- (3) (a) Han, R. *Stem Cells* **1994**, *12*, 53–63; (b) Alvi, K. A.; Pu, H.; Luche, M.; Rice, A.; App, H.; McMahon, G.; Dare, H.; Margolis, B. *J. Antibiot.* **1999**, *52*, 215–223; (c) Wang, X. W. *Drugs Future* **1999**, *24*, 613–617; (d) Stahl, P.; Kissau, L.; Mazitschek, R.; Huwe, A.; Furet, P.; Giannis, A.; Waldmann, H. *J. Am. Chem. Soc.* **2001**, *123*, 11586–11593; (e) Stahl, P.; Kissau, L.; Mazitschek, R.; Giannis, A.; Waldmann, H. *Angew. Chem., Int. Ed.* **2002**, *41*, 1174–1178; *Angew. Chem.* **2002**, *114*, 1222–1226.
- (4) Haraguchi, H.; Yokohama, K.; Oike, S.; Ito, M.; Nozaki, H. *Arch. Microbiol.* **1997**, *167*, 6–10.
- (5) Pérez-Sacau, E.; Estévez-Braun, A.; Ravelo, A. G.; Yapu, D. G.; Turba, A. G. *Chem. Biodiversity* **2005**, *2*, 264–274.
- (6) Campostakaki, G. M.; Steiman, R.; Seigle-Murandi, F.; Silva, A. A.; Bieber, L. *Rev. Microbiol.* **1992**, *23*, 106–111.
- (7) (a) DeSimone, R. W.; Currie, K. S.; Mitchell, S. A.; Darrow, J. W.; D. Pippin, A. *Comb. Chem. High Throughput Screening* **2004**, *7*, 473–491. (b) Li, J.; Liu, K. K. C. *Mini-Rev. Med. Chem.* **2004**, *4*, 207–233. (c) Li, J.; Liu, K.; Sakya, S. *Mini-Rev. Med. Chem.* **2005**, *5*, 1133–1144. (d) Costantino, L.; Barlocco, D. *Curr. Med. Chem.* **2006**, *13*, 65–85.
- (8) (a) Driscoll, J. S.; Hazard, G. F.; Wood, H. B.; Golden, A. *Cancer Chemother. Rep. Part 2* **1974**, *4*, 1–27. (b) Liu, K. K. C.; Li, J.; Sakya, S. *Mini-Rev. Med. Chem.* **2004**, *4*, 1105–1125. (c) Jiménez-Alonso, S.; Estévez-Braun, A.; Zárate, R.; Ravelo, A. G.; López, M. *Tetrahedron* **2007**, *63*, 3066–3074. (d) Jiménez-Alonso, S.; Chávez-Orellana, H.; Estévez-Braun, A.; Ravelo, A. G.; Feresin, G.; Tapia, A. *Tetrahedron* **2008**, *64*, 8938–8942. (e) Jiménez-Alonso, S.; Chávez-Orellana, H.; Estévez-Braun, A.; Ravelo, A. G.; Pérez-Sacau, E.; Machín, F. *J. Med. Chem.* **2008**, *51*, 6761–6772. (f) Jiménez-Alonso, S.; Pérez-Lomas, A. L.; Estévez-Braun, A.; Muñoz-Martínez, F.; Chávez-Orellana, H.; Ravelo, A. G.; Gamarro, F.; Castanys, S.; López, M. *J. Med. Chem.* **2008**, *51*, 7132–7143.
- (9) (a) Wardman, P. In *Selective Activation of Drugs by Redox Processes*; Adams, G. E., Breccia, A., Fielden, E. M., Wardman, P., Eds.; Plenum Press: New York, 1990; p 110. (b) Bard, A. J.; Faulkner, R. L. In *Electrochemical Methods, Fundamentals and Applications*; John Wiley and Sons: New York, 2003. (c) Hillard, E. A.; Caxico de Abreu, F.; Melo Ferreira, D. C.; Jaouen, G.; Goulart, M. O. F.; Amatore, C. *Chem. Commun.* **2008**, 2612–2628.
- (10) (a) Hammerich, O. In *Organic Electrochemistry*; Lund, H., Hammerich, O., Eds.; Marcel Dekker, Inc.: New York, 2001; p 95. (b) Amatore, C. In *Organic Electrochemistry*; Lund, H., Hammerich, O., Eds.; Marcel Dekker, Inc.: New York, 2001; p 1.
- (11) Begleiter, A.; Leith, M. K. *Cancer Res.* **1990**, *50*, 2872–2876.
- (12) (a) Hammerich, O.; Svensmark, B. In *Organic Electrochemistry*, 3rd ed.; Lund, H., Baizer, M. M., Eds.; Marcel Dekker: New York, 1991; p 16. (b) Chambers, J. Q. In *The Chemistry of the Quinonoid Compounds*; Patai, S., Rappoport, Z., Eds.; Wiley, New York, 1988; Vol. II, chapter 12, p 719.
- (13) (a) In *Function of Quinones in Energy Conserving Systems*; Trumpower, B. L., Ed.; Academic Press: New York, 1982. (b) Thurnauer, M. C.; Brown, J. W.; Gast, P.; Feezel, L. L. *Radiat. Phys. Chem.*

- 1989, 34, 647–651. (c) Van der Est, A. *Biochim. Biophys. Acta* **2001**, 1507, 212–225. (d) Rigby, S. E. J.; Evans, M. C. W.; Heathcote, P. *Biochim. Biophys. Acta* **2001**, 1507, 247–259. (e) Blankenship, R. E. In *Molecular Mechanisms of Photosynthesis*, 1st ed.; Blackwell Science: Oxford, 2002. (f) Voet, D.; Voet, J. G. In *Biochemistry*, 3rd ed.; Wiley: New York, 2004. (g) Epel, B.; Niklas, J.; Sinnecker, S.; Zimmermann, H.; Lubitz, W. *J. Phys. Chem. B* **2006**, 110, 11549–11560.
- (14) (a) Shiah, S. G.; Chuang, S. E.; Chau, Y. P.; Shen, S. C.; Kuo, M. L. *Cancer Res.* **1999**, 59, 391–398. (b) Waris, G.; Ahsan, H. *J. Carcinog.* **2006**, 5, 14.
- (15) Reichardt, C. In *Solvents and Solvent Effects in Organic Chemistry*, 3rd ed.; Wiley-VCH Verlag GmbH & Co. KGaA: Weinheim, 2003; chapter 6, pp 329–388.
- (16) Khajehpour, M.; Welch, C. M.; Kleiner, K. A.; Kauffman, J. F. *J. Phys. Chem. A* **2001**, 105, 5372–5379.
- (17) Sasirekha, V.; Vanelle, P.; Terme, T.; Meenakshi, C.; Umadevi, M.; Ramakrishnan, V. *J. Fluoresc.* **2007**, 17, 528–539.
- (18) Teimouri, M. B.; Khavasi, H. R. *Tetrahedron* **2007**, 63, 10269–10275.
- (19) (a) Perez-Sacau, E.; Diaz-Peñate, R. G.; Estevez-Braun, A.; Ravelo, A. G.; Garcia-Castellano, J. M.; Pardo, L.; Campillo, M. *J. Med. Chem.* **2007**, 50, 696–706. (b) Zakharova, O. D.; Ovchinnikova, L. P.; Goryunov, L. I.; Troshkova, N. M.; Shteingarts, V. D.; Nevinsky, G. A. *Eur. J. Med. Chem.* **2010**, 45, 2321–2326. (c) Kanaan, Y. M.; White, D. F.; Das, J. R.; Berhe, S.; Bakare, O.; Kenguele, H.; Beyene, D.; Zhou, Y.; Day, A. A.; Copeland, R. L. *Anticancer Res.* **2010**, 30, 519–528. (d) Bonifazi, E. L.; Rios-Luci, C.; Leon, L. G.; Burton, G.; Padron, J. M.; Misico, R. I. *Bioorg. Med. Chem.* **2010**, 18, 2621–2630.
- (20) (a) Tonholo, J.; Freitas, L. R.; de Abreu, F. C.; Azevedo, D. C.; Zani, C. L.; de Oliveira, A. B.; Goulart, M. O. F. *J. Braz. Chem. Soc.* **1998**, 9, 163–169. (b) Hillard, E. A.; Caxico de Abreu, F.; Melo Ferreira, D. C.; Jaouen, G.; Goulart, M. O. F.; Amatore, C. *Chem. Commun.* **2008**, 2612–2628.
- (21) Stallings, M. D.; Morrison, M. M.; Sawyer, D. T. *Inorg. Chem.* **1981**, 20, 2655–2660.
- (22) (a) Kuder, J. E.; Wychick, D.; Miller, R. L.; Walker, M. S. *J. Phys. Chem.* **1974**, 78, 1714–1718. (b) Russel, C.; Jaenicke, W. *J. Electroanal. Chem.* **1986**, 199, 139–151. (c) Crawford, P. W.; Carlos, E.; Ellegood, J. C.; Cheng, C. C.; Dong, Q.; Liu, D. F.; Luo, Y. L. *Electrochim. Acta* **1996**, 41, 2399–2403.
- (23) Jensen, B. S.; Parker, V. D. *J. Chem. Soc., Chem. Commun.* **1974**, 367–368.
- (24) Ashnagar, A.; Bruce, P. L.; Dutton, P. L.; Prince, R. C. *Biochim. Biophys. Acta* **1984**, 801, 351–359.
- (25) Inbaraj, J. J.; Krishna, M. C.; Gandhidasan, R.; Murugesan, R. *Biochim. Biophys. Acta* **1999**, 1472, 462–470.
- (26) (a) Cotterill, A. S.; Moody, C. J.; Mortimer, R. J.; Norton, C. L.; O'Sullivan, N.; Stephens, M. A.; Stradiotto, N. R.; Swann, E.; Stratford, I. J. *J. Med. Chem.* **1994**, 37, 3834–3843. (b) Qabaja, G.; Jones, G. B. *J. Org. Chem.* **2000**, 65, 7187–7194. (c) Qabaja, G.; Perchellet, E. M.; Perchellet, J. P.; Jones, G. B. *Tetrahedron Lett.* **2000**, 41, 3007–3010.
- (27) (a) Kunz, K. R.; Iyengar, B. S.; Dorr, R. T.; Alberts, D. S.; Remers, W. A. *J. Med. Chem.* **1991**, 34, 2281–2286. (b) Goulart, M. O. F.; Zani, C. L.; Tonholo, J.; Freitas, L. R.; de Abreu, F. C.; Oliveira, A. B.; Raslan, D. S.; Starling, S.; Chiari, E. *Bioorg. Med. Chem. Lett.* **1997**, 7, 2043–2048.
- (28) (a) Kamlet, M. J.; Taft, R. W. *J. Am. Chem. Soc.* **1976**, 98, 377–383. Taft, R. W.; Kamlet, M. J. *J. Am. Chem. Soc.* **1976**, 98, 2886–2894. (b) Taft, R. W.; Kamlet, M. J.; Abboud, J. L. *J. Am. Chem. Soc.* **1977**, 99, 6027–6038. (c) Kamlet, M. J.; Abboud, J. L. M.; Taft, R. W. *Prog. Phys. Org. Chem.* **1981**, 13, 485–630. (d) Taft, R. W.; Kamlet, M. J.; Abboud, J. L. M. *J. Am. Chem. Soc.* **1981**, 103, 1080–1086. (e) Marcus, Y. *Chem. Soc. Rev.* **1993**, 22, 409–416. (f) Laurence, C.; Nicolet, P.; Dalati, M. T.; Abboud, J. L. M.; Notario, R. *J. Phys. Chem.* **1994**, 98, 5807–5816. (g) Abboud, J. L. M.; Notario, R. *Pure Appl. Chem.* **1999**, 71, 645–718.
- (29) Ratera, I.; Sporer, C.; Ruiz-Molina, D.; Ventosa, N.; Baggerman, J.; Brouwer, A. M.; Rovira, C.; Veciana, J. *J. Am. Chem. Soc.* **2007**, 129, 6117–6129.
- (30) Gutierrez, P. L. Nguyen, B. In *Redox Chemistry and Interfacial Behaviour of Biological Molecules*; Dryhurst, G., Niki, K., Eds.; Plenum Press: New York, 1988, pp 369–382.
- (31) Sutovsky, Y.; Likhtenshtein, G. I.; Bittner, S. *Tetrahedron* **2003**, 59, 2939–2945.
- (32) Ventosa, N.; Ruiz-Molina, D.; Sedó, J.; Rovira, C.; Tmas, S.; André, J. J.; Bibier, A.; Veciana, J. *Chem.—Eur. J.* **1999**, 5, 3533–3548.